Downlink Throughput Performance of Distributed Antenna Network Using Transmit/Receive Diversity

Ryusuke MATSUKAWA† Tatsunori OBARA† Kazuki TAKEDA† and Fumiyuki ADACHI‡
Dept. of Electrical and Communication Engineering, Graduate School of Engineering, Tohoku University
6-6-05 Aza-Aoba, Aramaki, Aoba-ku, Sendai, 980-8579 Japan
E-mail: † {matsukawa, obara, kazuki}@mobile.ecei.tohoku.ac.jp, ‡ adachi@ecei.tohoku.ac.jp

Abstract—**In this paper, we investigate how a distributed antenna network (DAN) offers better throughput performance than a conventional cellular network (CN). In DAN, a group of multiple antennas are distributed in each cell of the CN in order to mitigate the adverse effect of path loss. Moreover, antenna diversity technique can make use of shadowing and multipath fading to improve the transmission performance due to a large spatial diversity gain. In this paper, we consider frequency-domain space-time block coded-joint transmit/ receive diversity (FD-STBC-JTRD) for downlink transmission of single-carrier (SC) DAN. FD-STBC-JTRD uses frequency-domain pre-equalization (pre-FDE) instead of receive FDE to keep the mobile terminal's complexity low, and achieves the full-diversity gain. We show by computer simulation that the transmit power for achieving the required throughput can be significantly reduced compared to the conventional CN.**

Keywords-distributed antenna network; space-time block coding; pre-equalization; HARQ

I. INTRODUCTION

In the broadband wireless data transmissions, the propagation channel becomes severely frequency-selective [1]. The bit error rate (BER) performance of broadband single-carrier (SC) transmissions is seriously degraded due to strong inter-symbol interference (ISI) resulting from channel frequency-selectivity. Frequency-domain equalization (FDE) is one of the solutions to overcome the ISI problem. Minimum mean square error based FDE (MMSE-FDE) can take advantage of the channel frequency-selectivity and obtain large frequency diversity gain [2, 3]. However, the received signal power may drop due to distance-dependent path loss and log-normally distributed shadowing loss according to the movement of the mobile terminal (MT) [4]. In conventional cellular networks (CNs), the service area is covered by many cells with a base station (BS) in each cell. The transmission quality severely degrades when MT approaches the cell edge. Although transmit and/or receive antenna diversity is a powerful technique to mitigate the effect of frequency-selective fading [5-8], the received signal power degrades due to path and shadowing losses.

To mitigate the problems arising from frequency-selective fading, shadowing loss, and path loss, we have been studying the potential of a distributed antenna network (DAN) [9-11]. Figure 1 illustrates the conceptual structure of the DAN. In the DAN, a number of antennas are distributed in each cell. The conventional BS is replaced by a signal processing center (SPC) and each distributed antenna is connected to the SPC by an optical link. Some of the distributed antennas, which are close to a MT, cooperatively serve the MT using transmit diversity technique to mitigate the effects of path and shadowing losses as well as frequency-selective fading.

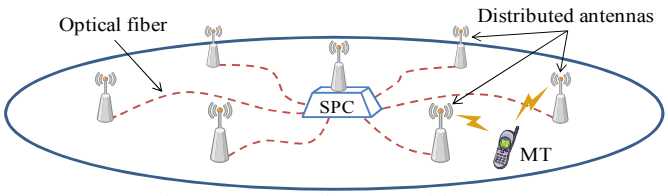

Figure 1. Conceptual structure of the DAN.

Recently, authors have proposed a frequency-domain space-time block coded-joint transmit/receive diversity (FD-STBC-JTRD) with pre-FDE [7,8], which achieves the maximal ratio diversity gain. FD-STBC-JTRD requires channel state information (CSI) at the transmitter while at the receiver it requires only addition, subtraction and conjugate operations (i.e., the signal processing at the receiver becomes simpler). FD-STBC-JTRD can use an arbitrary number of transmit antennas without decreasing the coding rate. However, the coding rate decreases to less 1 when more than 2 receive antennas are used. Therefore, FD-STBC-JTRD is suitable for downlink transmissions; large antenna diversity gain can be obtained by using an arbitrary number of distributed antennas while alleviating the complexity problem at MTs.

In our previous work, we showed that SC-DAN using FD-STBC-JTRD significantly improves the outage BER performance [11]. However, the throughput performance of FD-STBC-JTRD using hybrid automatic repeat request (HARQ) has not been studied yet. In this paper, assuming HARQ with incremental redundancy (IR) strategy [12-14], we will investigate by computer simulation the throughput distribution of FD-STBC-JTRD downlink in SC-DAN. We will discuss the impact of the number of transmit/receive antennas on the throughput performance and show that the DAN significantly reduces the transmit power for achieving the required throughput compared to a conventional CN.

The remainder of this paper is organized as follows. Section II describes the system models. Section III introduces the transmitter/receiver structures for FD-STBC-JTRD downlink using HARQ-IR in SC-DAN. Section IV shows the computer simulation results on the outage throughput performance. Finally, Section V offers some conclusions and future work.

978-1-4244-8325-9/11/$26.00 ©2011 IEEE

II. SYSTEM MODEL

A. Channel model

N_{total} distributed antennas are deployed in a cell and a MT is equipped with N_r receive antennas. In this paper, N_{total}=7 and N_r=1~3 are considered. N_t distributed antennas are selected among N_{total} distributed antennas for the downlink packet access. The propagation channel is characterized by distance-dependent path loss, log-normally distributed shadowing loss, and frequency-selective fading channel composed of symbol-spaced L discrete paths. The impulse response of a frequency-selective fading channel between the n-th distributed antenna and the m-th MT antenna can be expressed as

$$h_{m,n}(\tau) = \sum_{l=0}^{L-1} h_{m,n,l}\delta(\tau - \tau_l), \quad (1)$$

where $h_{m,n,l}$ and τ_l are the complex-valued channel gain with $E[\Sigma_{l=0}^{L-1}|h_{m,n,l}|^2]$=1 and the time delay of the l-th path, respectively. The instantaneous received signal power per MT receive antenna, $P_{r,n}$, is given by

$$P_{r,n} = p_{t,n} \cdot r_n^{-\alpha} \cdot 10^{-\frac{\eta_n}{10}} \cdot \frac{1}{N_r} \sum_{m=0}^{N_r-1} \sum_{l=0}^{L-1} \left|h_{m,n,l}\right|^2, \quad (2)$$

where $p_{t,n}$ represents the transmit power from the n-th antenna, r_n represents the distance between the n-th distributed antenna and the MT, and α and η_n are respectively the path loss exponent and the shadowing loss in dB. η_n is a zero-mean Gaussian variable with standard deviation σ. Denoting that the cell radius is R and substituting $P_{t,n}$=$p_{t,n}$·$R^{-\alpha}$ and R_n=r_n/R into Eq. (2), the received power can be rewritten as

$$P_{r,n} = P_{t,n} \cdot R_n^{-\alpha} \cdot 10^{-\frac{\eta_n}{10}} \cdot \frac{1}{N_r} \sum_{m=0}^{N_r-1} \sum_{l=0}^{L-1} \left|h_{m,n,l}\right|^2, \quad (3)$$

where $P_{t,n}$ and R_n denote the normalized transmit power and the normalized distance. The total transmit power from N_t distributed antennas is kept constant as P_t=$\Sigma_{n=0}^{N_t-1} P_{t,n}$.

B. System model

In this paper, a single MT and single cell model is considered. Figure 2 illustrates the models of DAN with N_{total}=7 distributed antennas and CN with N_{total}=7 localized antennas. The cell radius is normalized to 1. N_{total} distributed antennas are equidistantly arranged on the circle of normalized radius R=2/3. They are connected to the SPC by optical links (ideal signal transmission between each distributed antenna and the SPC is assumed). The value of $\Sigma_{l=0}^{L-1}|h_{m,n,l}|^2$ approaches unity for a large number of propagation paths (L>>1) according to the law of large numbers [1]. Eq. (3) can be approximated as

$$P_{r,n} \approx P_{t,n} \cdot R_n^{-\alpha} \cdot 10^{-\frac{\eta_n}{10}}, \quad (4)$$

which represents the local average received signal power. In DAN, N_t distributed antennas are selected from N_{total} antennas according to the descending order of the local average received signal power. In CN, N_{total} antennas localized at the BS are selected according to the descending order of the channel gain (i.e., $\Sigma_{l=0}^{L-1}|h_{m,n,l}|^2$) because the path and shadowing losses are the same for all of N_{total} antennas.

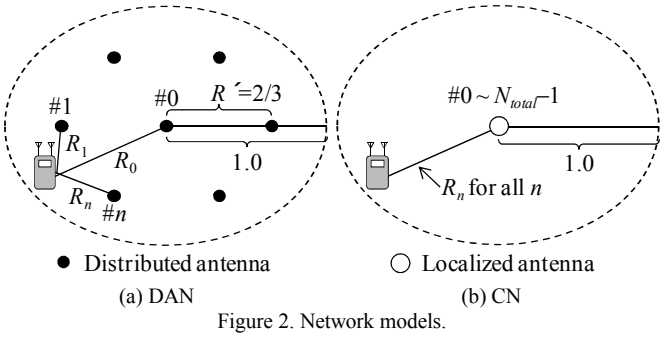

Figure 2. Network models.

III. HARQ-IR FOR FD-STBC-JTRD DOWNLINK

Figure 3 illustrates the transmitter/receiver structures of the FD-STBC-JTRD using HARQ for downlink. If any errors are detected at the MT, a NACK signal is sent to the SPC to request the retransmission. Then, transmitted packets are combined using log-likelihood ratio (LLR) and the error detection is performed again. If there are no errors, the MT sends an ACK to request the new packet transmission. In this paper, turbo-coded HARQ-IR using type-II S-P2 [12-14] is considered. The following puncture matrices are used:

$$I_0 = \begin{pmatrix} 1 & 1 \\ 0 & 0 \\ 0 & 0 \end{pmatrix}, I_1 = \begin{pmatrix} 0 & 0 \\ 1 & 0 \\ 0 & 1 \end{pmatrix}, I_2 = \begin{pmatrix} 0 & 0 \\ 0 & 1 \\ 1 & 0 \end{pmatrix}. \quad (5)$$

The q-th retransmission uses the puncture matrix I_i with i=q mod 3, where q=0 represents the initial transmission. The i=0th transmission consists of only the systematic bit sequence. The i=1 and 2th transmissions consist of parity bits which are generated by rate-1/3 turbo encoder and the puncture matrices I_1 and I_2.

Then, the turbo-coded bit sequence is data modulated and FD-STBC-JTRD encoding is performed for the transmission. In the following, the operation principle of FD-STBC-JTRD is presented. Without the loss of generality, a block transmission of J×N_c data modulated symbols $\{d(t);\ t=0\sim JN_c-1\}$ is considered, where J and N_c are an positive integer.

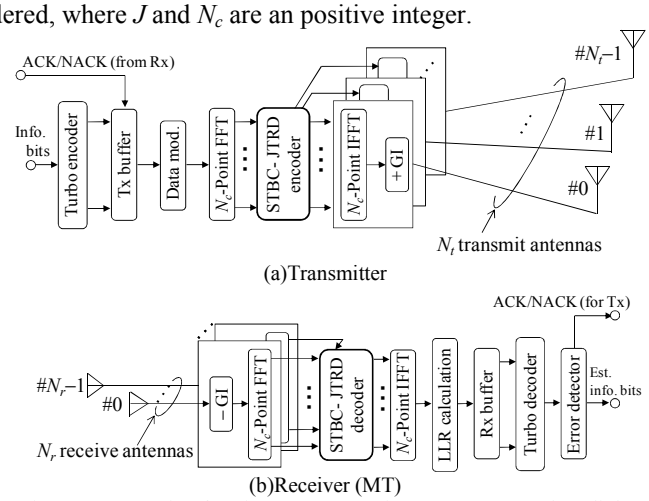

Figure 3. Transmitter/receiver structures of FD-STBC-JTRD downlink.

A. Transmission procedure

A sequence of $J \times N_c$ data modulated symbols to be transmitted is divided into a sequence of J blocks of N_c symbols each. N_c-point fast Fourier transform (FFT) is applied to decompose the j-th block $\{d_j(t);\ t=0\sim N_c-1\}$ into the frequency-domain signal $\{D_j(k);\ k=0\sim N_c-1\}$ as

$$D_j(k) = \frac{1}{\sqrt{N_c}} \sum_{t=0}^{N_c-1} d_j(t) \exp\left(-j2\pi k \frac{t}{N_c} \right). \quad (6)$$

A sequence of J frequency-domain signal blocks, $\{D_j(k);\ k=0\sim N_c-1,\ j=0\sim J-1\}$, is encoded into N_t streams of Q encoded frequency-domain signal blocks each, as shown in Fig. 4. A combination of J and Q is shown in Table I for $N_r=1\sim3$. The space-time coding rate R_{stbc} (= J/Q) decreases to 3/4 for $N_r=3$.

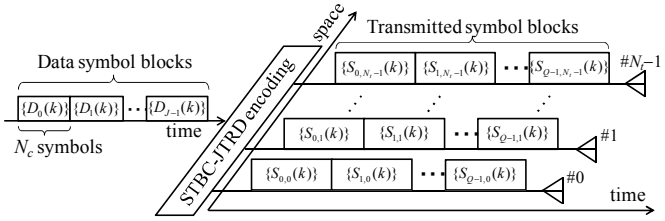

Figure 4. FD-STBC-JTRD encoding.

TABLE I. RELATIONSHIP OF N_r, J, Q, AND CODE RATE R_{stbc}

N_r	J	Q	R_{stbc}
1	1	1	1
2	2	2	1
3	3	4	3/4

N_t streams of encoded signal blocks is represented using the matrix form as

$$\begin{aligned} \mathbf{S}(k) &= [\mathbf{S}_0(k),...,\mathbf{S}_q(k),...,\mathbf{S}_{Q-1}(k)] \\ &= C_{N_r} \mathbf{W}^H(k) \mathbf{D}_{N_r}(k) \end{aligned}. \quad (7)$$

In Eq. (7), $\mathbf{S}_q(k)=[S_{q,0}(k),\ldots,S_{q,n}(k),\ldots,S_{q,N_t-1}(k)]^T$ is the q-th encoded frequency-domain signal vector at the k-th frequency and $\mathbf{W}(k)=[\mathbf{W}_0(k),\ldots,\ \mathbf{W}_m(k),\ldots,\ \mathbf{W}_{N_r-1}(k)\ ]$ with $\mathbf{W}_m(k)=[W_{m,0}(k),\ldots,W_{m,n}(k),\ldots,\ W_{m,N_t-1}(k)\ ]$ is an $N_r \times N_t$ transmit FDE weight matrix, where $W_{m,n}(k)$ is given by [8]

$$W_{m,n}(k) = A(k) \cdot H_{m,n}(k) \quad (8)$$

with

$$A(k) = \frac{1}{\frac{1}{N_r} \sum_{m=0}^{N_r-1} \sum_{n=0}^{N_t-1} \left| H_{m,n}(k) \right|^2 + \left(\frac{E_s}{N_0} \right)^{-1}}, \quad (9)$$

and $(.)^H$ is the Hermitian transpose operation. $H_{m,n}(k)$ represents the channel gain at the k-th frequency between the n-th distributed antenna and the m-th MT antenna, given as

$$H_{m,n}(k) = \sqrt{R_n^{-\alpha} \cdot 10^{-\frac{\eta_n}{10}}} \sum_{l=0}^{L-1} h_{m,n,l} \exp\left(-j2\pi k \frac{\tau_l}{N_c} \right). \quad (10)$$

C_{N_r} is the power normalization factor to keep the average of the total transmit power intact, given as

$$C_{N_r} = \sqrt{\frac{N_c}{\sum_{m=0}^{N_r-1} \sum_{n=0}^{N_t-1} \sum_{k=0}^{N_c-1} \left| W_{m,n}(k) \right|^2}}. \quad (11)$$

$\mathbf{D}_{N_r}(k)$ is the $N_r \times Q$ space-time encoding matrix [8] and is given as

$$\mathbf{D}_1(k) = D_0(k) \quad \ldots \text{ for } N_r = 1, \quad (12a)$$

$$\mathbf{D}_2(k) = \begin{pmatrix} D_0(k) & -D_1^*(k) \\ D_1(k) & D_0^*(k) \end{pmatrix} \quad \ldots \text{ for } N_r = 2, \quad (12b)$$

$$\mathbf{D}_3(k) = \begin{pmatrix} D_0(k) & -D_1^*(k) & -D_2^*(k) & 0 \\ D_1(k) & D_0^*(k) & 0 & D_2(k) \\ D_2(k) & 0 & D_0^*(k) & -D_1(k) \end{pmatrix} \quad \ldots \text{ for } N_r = 3. \quad (12c)$$

Finally, N_c-point inverse FFT (IFFT) is applied to $\mathbf{S}(k)$ to obtain the time-domain codeword $\{s_{q,n}(t);\ t=0\sim N_c-1\}$, $q=0\sim Q-1$ and $n=0\sim N_t-1$, as

$$s_{q,n}(t) = \sqrt{\frac{2P_t}{N_c}} \sum_{k=0}^{N_c-1} S_{q,n}(k) \exp\left(j2\pi \frac{k}{N_c} \right), \quad (13)$$

where $P_t=E_s/T_s$ with E_s and T_s denote the symbol energy and the symbol length, respectively. After inserting a cyclic prefix (CP) of N_g symbols into the guard interval (GI), N_t streams of Q blocks each are transmitted from N_t distributed antennas.

B. Reception procedure

At the MT, a superposition of N_t transmitted signals is received by N_r receive antennas. After removing the GI, received signals are transformed by N_c-point FFT into the received frequency-domain signals $\{R_{q,m}(k);\ k=0\sim N_c-1\}$, $q=0\sim Q-1$ and $m=0\sim N_r-1$, which can be expressed using the matrix form as

$$\begin{aligned} \mathbf{R}(k) &= [\mathbf{R}_0(k),...,\mathbf{R}_q(k),...,\mathbf{R}_{Q-1}(k)] \\ &= \sqrt{2P_t} \mathbf{H}(k) \mathbf{S}(k) + \mathbf{N}(k) \end{aligned}, \quad (14)$$

where $\mathbf{R}_q(k)=[R_{q,0}(k),\ldots,R_{q,m}(k),\ldots,\ R_{q,N_r-1}(k)\ ]^T$ and $\mathbf{H}(k)=[\mathbf{H}_0(k),\ldots,\mathbf{H}_m(k),\ldots,\ \mathbf{H}_{N_r-1}(k)\ ]^T$ with $\mathbf{H}_m(k)=[H_{m,0}(k),\ldots,H_{m,n}(k),\ \ldots,\ H_{m,N_t-1}(k)\ ]^T$. $\mathbf{N}(k)=[\mathbf{N}_0(k),\ldots,\mathbf{N}_m(k),\ldots,\mathbf{N}_{N_r-1}(k)\ ]^T$ is the noise matrix with its m-th column vector $\mathbf{N}_m(k)=[N_{m,0}(k),\ldots,\ N_{m,q}(k),\ldots,N_{m,Q-1}(k)]$, where $\{N_{m,q}(k)\}$ are i.i.d. complex Gaussian variables having zero mean and variance $2N_0/T_s$ with N_0 being the single-sided power spectrum density of additive white Gaussian noise (AWGN). FD-STBC-JTRD decoding is carried out on $\mathbf{R}(k)$ to obtain the frequency-domain soft-decision signal vector $\hat{\mathbf{D}}_{N_r}(k)=[\ \hat{D}_0(k),\ldots,\ \hat{D}_j(k)\ ,\ldots,\hat{D}_{J-1}(k)\ ]^T$ as

$$\hat{\mathbf{D}}_1(k) = R_{0,0}(k) \quad \ldots \text{ for } N_r = 1, \quad (15a)$$

$$\hat{\mathbf{D}}_2(k) = \begin{pmatrix} R_{0,0}(k) + R_{1,1}^*(k) \\ R_{0,1}(k) - R_{1,0}^*(k) \end{pmatrix} \quad \ldots \text{ for } N_r = 2, \quad (15b)$$

$$\hat{\mathbf{D}}_3(k) = \begin{pmatrix} R_{0,0}(k) + R_{1,1}^*(k) + R_{2,2}^*(k) \\ R_{0,1}(k) - R_{1,0}^*(k) + R_{3,2}^*(k) \\ R_{0,2}(k) - R_{2,0}^*(k) - R_{3,1}^*(k) \end{pmatrix} \quad \ldots \text{ for } N_r = 3. \quad (15c)$$

As understood from Eq. (15), FD-STBC-JTRD decoding requires only addition/subtraction and conjugate operations. Eq. (15) can be rewritten as

$$\hat{\mathbf{D}}_{N_r}(k) = \sqrt{2P_t}\,A(k)\left(\sum_{m=0}^{N_r-1}\sum_{n=0}^{N_t-1}\left|H_{m,n}(k)\right|^2\right)\begin{pmatrix} D_0(k) \\ \vdots \\ D_{J-1}(k) \end{pmatrix} + \hat{\mathbf{N}}(k) \quad (16)$$

with J=1, 2, and 3 for N_r=1, 2, and 3, respectively, where $\hat{\mathbf{N}}(k)$ represents the equivalent noise vector with its J elements being independent complex-valued zero-mean Gaussian variables having variance $2N_rN_0/T_s$. It can be understood from Eq. (16) that FD-STBC-JTRD can achieve $N_r \times N_t$ -th full diversity gain. Finally, N_c-point IFFT is applied to transform $\{\hat{D}_j(k)\,;\, k=0\sim N_c-1\}$ into the time-domain soft decision symbol sequence $\{\hat{d}_j(t)\,;\, t=0\sim N_c-1\}$ as

$$\hat{d}_j(t) = \frac{1}{\sqrt{N_c}}\sum_{k=0}^{N_c-1}\hat{D}_j(k)\exp\left(j2\pi k\frac{t}{N_c}\right). \quad (17)$$

IV. Computer Simulation

A. Simulation condition

The computer simulation condition is summarized in Table II. Frequency-selective block Rayleigh fading is assumed, in which the channel stays constant during the transmission of a packet. The cumulative distribution function (CDF) of the throughput is measured by randomly changing the MT location in the cell. From the CDF, the 1%-outage throughput, below which the throughput falls at a probability of 1%, was obtained.

TABLE II. Simulation Condition

Transmitter	Data modulation	16QAM
	Block size	N_c=256
	Guard interval length	N_g=32
	No. of antennas in a cell	N_{total}=7
	No. of transmit antennas	N_t=1, 2, 4, 7
	Pre-FDE weight	MMSE
	Channel estimation	Ideal
HARQ	Packet size	1536 bits
	Turbo coding	Two (13, 15) RSC encoders
	Packet combining	IR (Type II S-P2)
	Decoder	Log MAP (8 iterations)
Channel model	Fading	Frequency-selective block Rayleigh
	Power delay profile	L=16-path uniform
	Time delay	$\tau_l = l$
	Path loss exponent	α=3.5
	Shadowing loss standard deviation	σ=7.0
Receiver	No. of receive antennas	N_r=1, 2

B. Impacts of N_t and N_r

Figure 5(a) plots the 1%-outage throughput of SC-DAN downlink using FD-STBC-JTRD and HARQ-IR as a function of the normalized transmit E_s/N_0 with N_r as a parameter. From Fig. 5(a), it can be seen that the 1%-outage throughput is maximized when N_r=2. There exists a tradeoff between the receive diversity gain and the space-time coding rate R_{stbc}. As N_r increases, larger receive diversity gain can be obtained, however, R_{stbc} decreases to 3/4 when N_r=3. As a consequence, N_r=2 provides the largest throughput.

Figure 5(b) plots the 1%-outage throughput of SC-DAN downlink using FD-STBC-JTRD and HARQ-IR as a function of the normalized transmit E_s/N_0 with N_t as a parameter. Comparison of Figs. 5(a) and 5(b) shows that increasing N_t achieves much higher throughput than increasing N_r. This is because larger spatial diversity gain can be achieved by increasing N_t. However, the use of more than N_t=4 provides only a marginal increase in the throughput. As N_t increases, more antennas which are not close to MT are selected. They do not contribute to the performance improvement since only a small portion of total transmit power is allocated to them. In the next subsection, $(N_t, N_r) = (4, 2)$ is used.

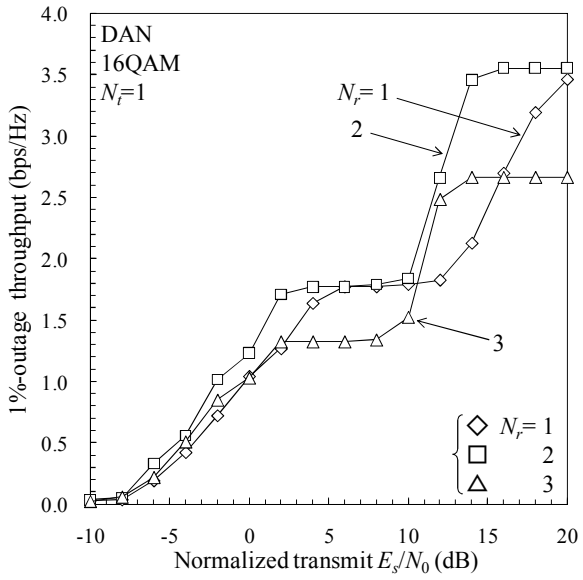

(a) Impact of N_r

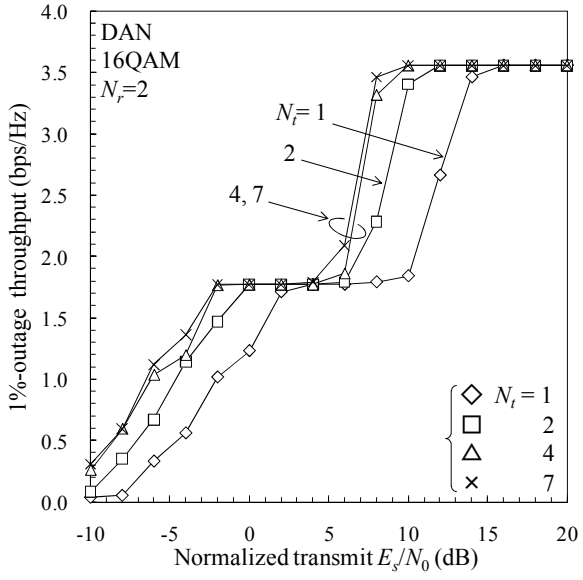

(b) Impact of N_t

Figure 5. Impacts of the numbers of transmit and receive antennas, N_t and N_r.

C. Comparison with CN

Figure 6 compares DAN and CN. DAN significantly improves 1%-outage throughput. For the given 1%-outage throughput, DAN can significantly reduce the transmit power compared to CN; for achieving a 1%-outage throughput of 3.56 bps/Hz, the transmit power can be reduced by about 16dB. This is because the effects of path and shadowing losses are suppressed by using distributed antennas.

The spatial distribution of the throughput in a cell is plotted in Fig. 7, for the normalized transmit E_s/N_0=0dB and (N_t, N_r) = (4, 2). Higher throughput is achieved over an entire area in DAN while the throughput drops at the cell edge in CN; the throughput at the cell edge is about 2.6 bps/Hz in DAN while it is about 1.2 bps/Hz in CN.

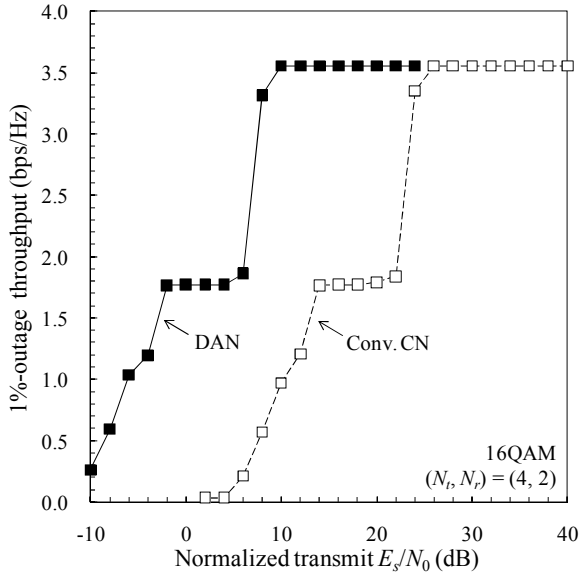

Figure 6. Comparison between DAN and CN.

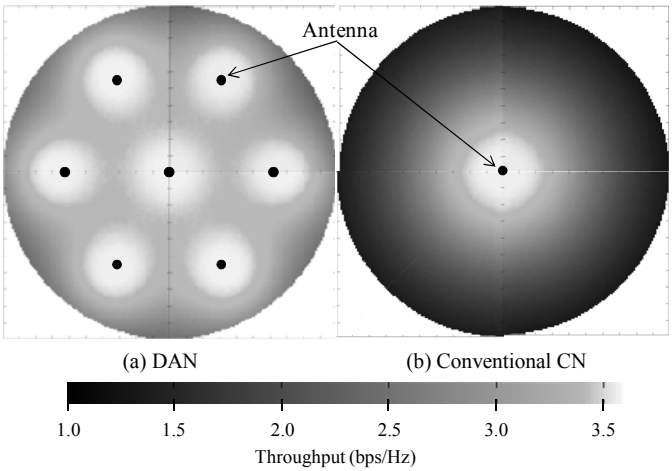

Figure 7. Spatial distribution of throughput with N_{total}=7.

V. Conclusion

In this paper, we investigated the throughput distributions of FD-STBC-JTRD downlink using HARQ-IR in SC-DAN. DAN can improve the outage throughput while keeping MT's complexity low. We showed that the DAN significantly reduces the transmit power to achieve the same throughput value compared to the CN. In this paper, we assumed the single-cell and single-user case. How much the FD-STBC-JTRD can suppress the co-channel interference (CCI) from other users and other cells is left as an important future study.

References

[1] W. C. Jakes, Jr., Ed., *Microwave Mobile Communications*. Wiley, New York, 1974.

[2] D. Falconer, S. L. Ariyavisitakul, A. Benyamin-Seeyar, and B. Eidson, "Frequency domain equalization for single-carrier broadband wireless systems," IEEE Commun. Mag., Vol.40, No. 4, pp. 58-66, Apr. 2002.

[3] F. Adachi, T. Sao and T. Itagaki, "Performance of multicode DS-CDMA using frequency domain equalization in a frequency selective fading channel," IEE Electronics Letters, Vol. 39, No.2, pp. 239-241, Jan. 2003.

[4] A. Goldsmith, *Wireless Communications*, Cambridge University Press, 2005.

[5] R. L. U Choi and R. D. Murch, "A transmit MIMO scheme with frequency domain pre-equalization for wireless frequency selective channels," IEEE Trans. Wireless Commun., Vol. 3, No. 3, pp. 929-938, May 2004.

[6] A. Gusmao, R. Dinis and N. Esteves,"On frequency-domain equalization and diversity combining for broadband wireless communications," IEEE Trans Wireless Commun., Vol. 51, No. 7, pp. 1029-1033, Jul. 2003.

[7] H. Tomeba, K. Takeda, and F. Adachi, "Space-time block coded-joint transmit/receive antenna diversity using more than 4 receive antennas," 2008 IEEE 68th Vehicular Technology Conference (VTC-Fall), Calgary, Canada, 21-25 September 2008.

[8] H. Tomeba and F. Adachi, "Frequency-domain space-time block coded-joint transmit/receive diversity for the single carrier transmission," Proc.10th IEEE International Conference on Communication Systems(ICCS 2006), Singapore, 30 Oct. - Nov. 2006.

[9] E. Kudoh and F. Adachi, "Study of a multi-hop communication in a virtual cellular system," Proc. 6th International Symposium on Wireless Personal Multimedia Communications (WPMC), Vol.3, pp.261-265, Yokosuka, Japan, 19-22 Oct. 2003.

[10] W. Choi, "Downlink performance and capacity of distributed antenna systems," IEEE Trans. Wireless Commun., Vol. 6, No. 1, pp. 69-73, Jan. 2007.

[11] R. Matsukawa, T. Obara, K. Takeda, and F. Adachi, "Single-carrier distributed antenna network downlink using joint transmit/receive diversity," Proc.12th IEEE International Conference on Communication Systems (ICCS 2010), Singapore, 17-20 Nov. 2010.

[12] C. Berrou, A. Glavieux, and P. Thitimajshima, "Near Shannon limit error-correcting coding and decoding; Turbo-codes. 1," IEEE International Conference on Communications (ICC), Vol. 2, pp. 1064-1070, Switzerland, May 1993.

[13] J. Hagenauer, "Rate-compatible punctured convolutional codes (RCPC codes) and their application," IEEE Trans. Commun., Vol. 36, No. 4, pp. 389-400, Apr. 1988.

[14] D. Garg, and F. Adachi, "Throughput comparison of turbo-coded HARQ in OFDM, MC-CDMA and DS-CDMA with frequency-domain equalization," IEICE Trans. Commun., Vol. E88-B, No.2, pp.664-677, Feb. 2005.